Supplementary Information

In-situ growth of Co_3O_4 nanoparticles on α-MnO_2 nanotubes: A new hybrid for high-performance supercapacitor

Dongbo Yu,[a,b] Jianfeng Yao,[a] Ling Qiu,[c] Yufei Wang,[c] Xinyi Zhang,[d] Yi Feng,[*b] and Huanting Wang[*a]

[a] Department of Chemical Engineering, Monash University, Clayton, Victoria 3800, Australia

[b] School of Materials Science and Engineering, Hefei University of Technology, Hefei, Anhui 230009, People's Republic of China

[c] Department of Materials Engineering, Monash University, Clayton, Victoria 3800, Australia

[d] School of Chemistry, Monash University, Clayton, Victoria 3800, Australia

E-mail addresses: huanting.wang@ monash.edu (H. Wang); fyhfut@126.com (Y. Feng)

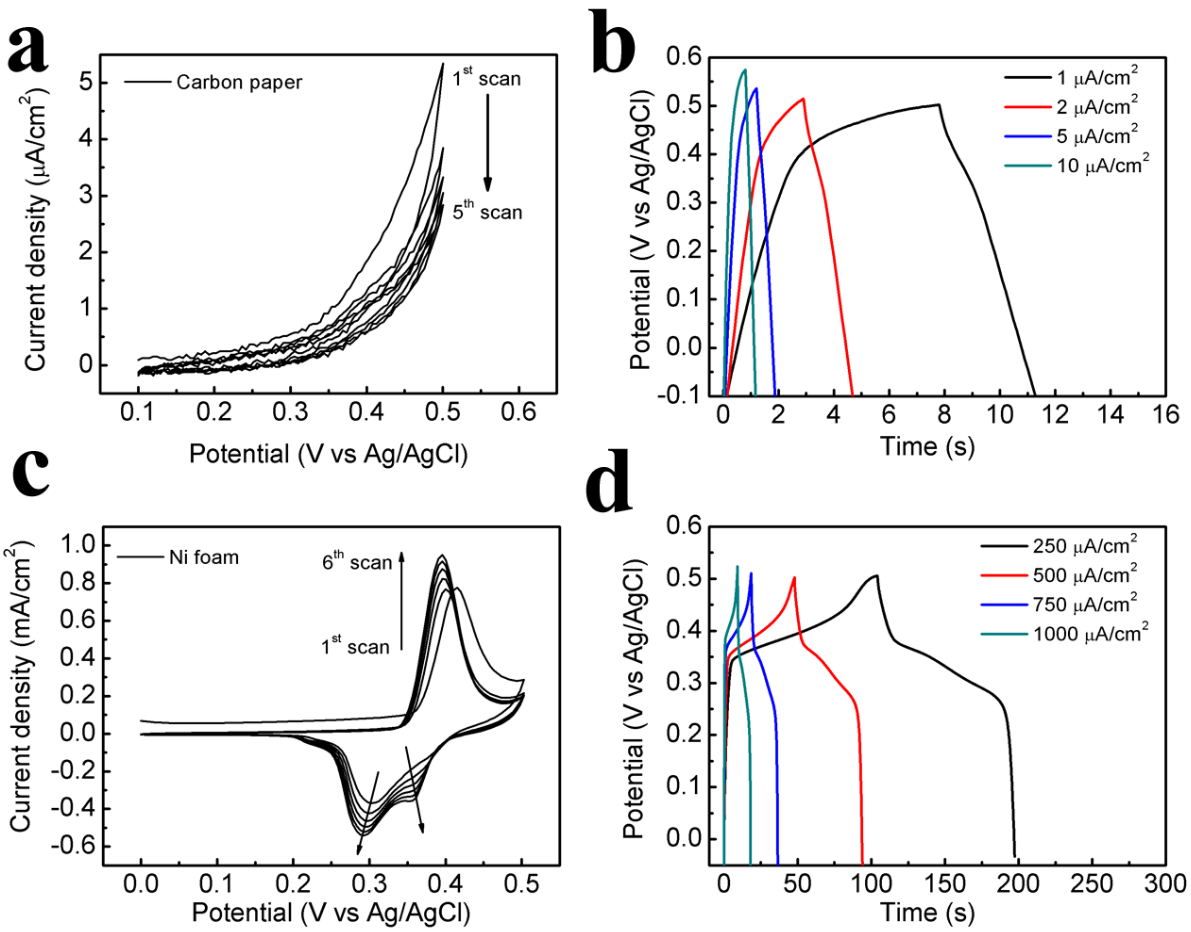

Fig. S1 Cyclic voltammetric curves (a) and galvanostatic charge-discharge curves (b) of carbon paper; cyclic voltammetric curves (c) and galvanostatic charge-discharge curves (d) of Ni foam. The current density of carbon paper decreased with the repeating scans. In contrary, repeating the cycles led to the increase of current density for Ni foam. Carbon paper hardly contributed to the capacitance, while Ni foam itself was active and gave very big contribution to the capacitance. The calculated capacitance of Ni foam devoted was about 20 F/(g·cm^2), 43 F/(g·cm^2), 92 F/(g·cm^2) and 188 F/(g·cm^2) as the loading amount of active materials was considered as 1 mg, 0.5 mg, 0.75 mg and 0.25 mg, respectively. According to the results, we could demonstrate that it was reasonable to use carbon paper as current collector rather than Ni foam when the loading amount of active materials was less than 1 mg. In our case, the loading amount was 0.8 mg.

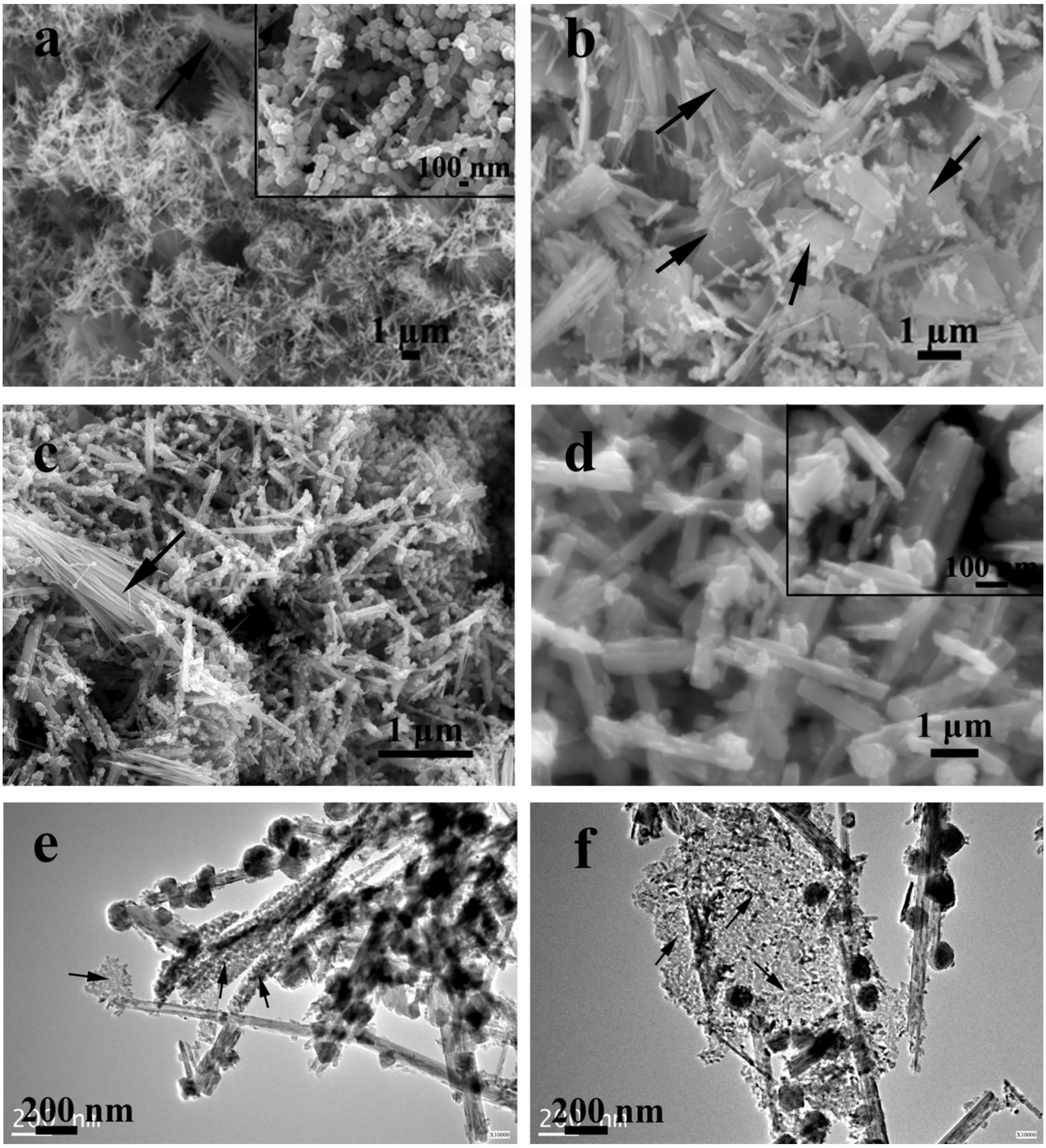

Fig S2 SEM images of obtained materials without the addition of NH_4F at high concentration (a-c) (the white arrows in (a-c) show the by-product generated in the synthesis) and low concentration (d) of the precursor solution. TEM images (e, f) of resulting products without the addition of NH_4F at high concentration (black arrows show nanowire clusters and nanofilms).

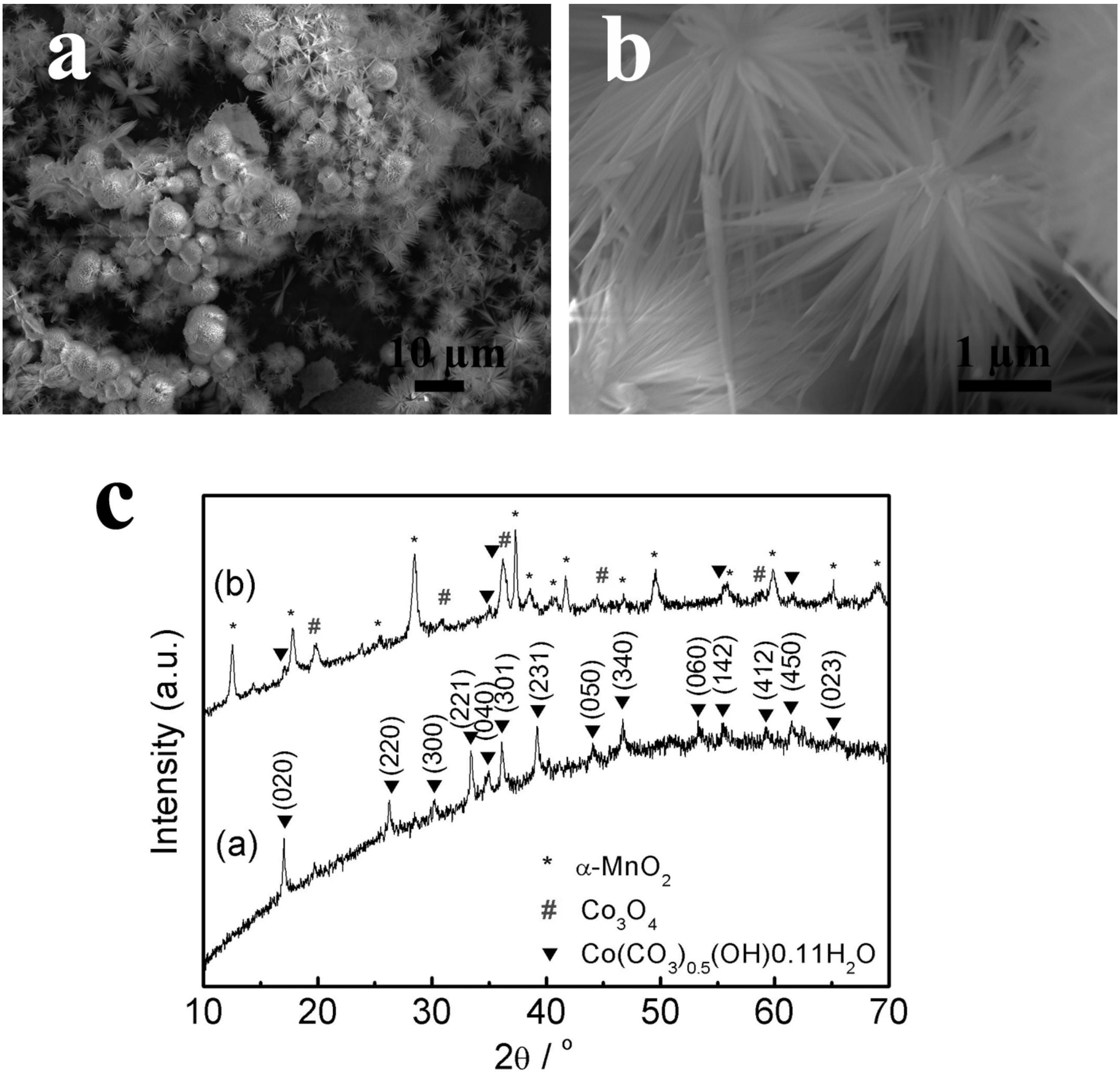

Fig S3 SEM images of products without the addition of α-MnO_2 nanotubes and NH_4F (a)(b). XRD of resulting materials without the addition of α-MnO_2 nanotubes and NH_4F (curve a) and without the addition of NH_4F (curve b). It indicates that the by-product contains $Co(CO_3)_{0.5}(OH)\cdot 0.11H_2O$ in the absence of NH_4F.

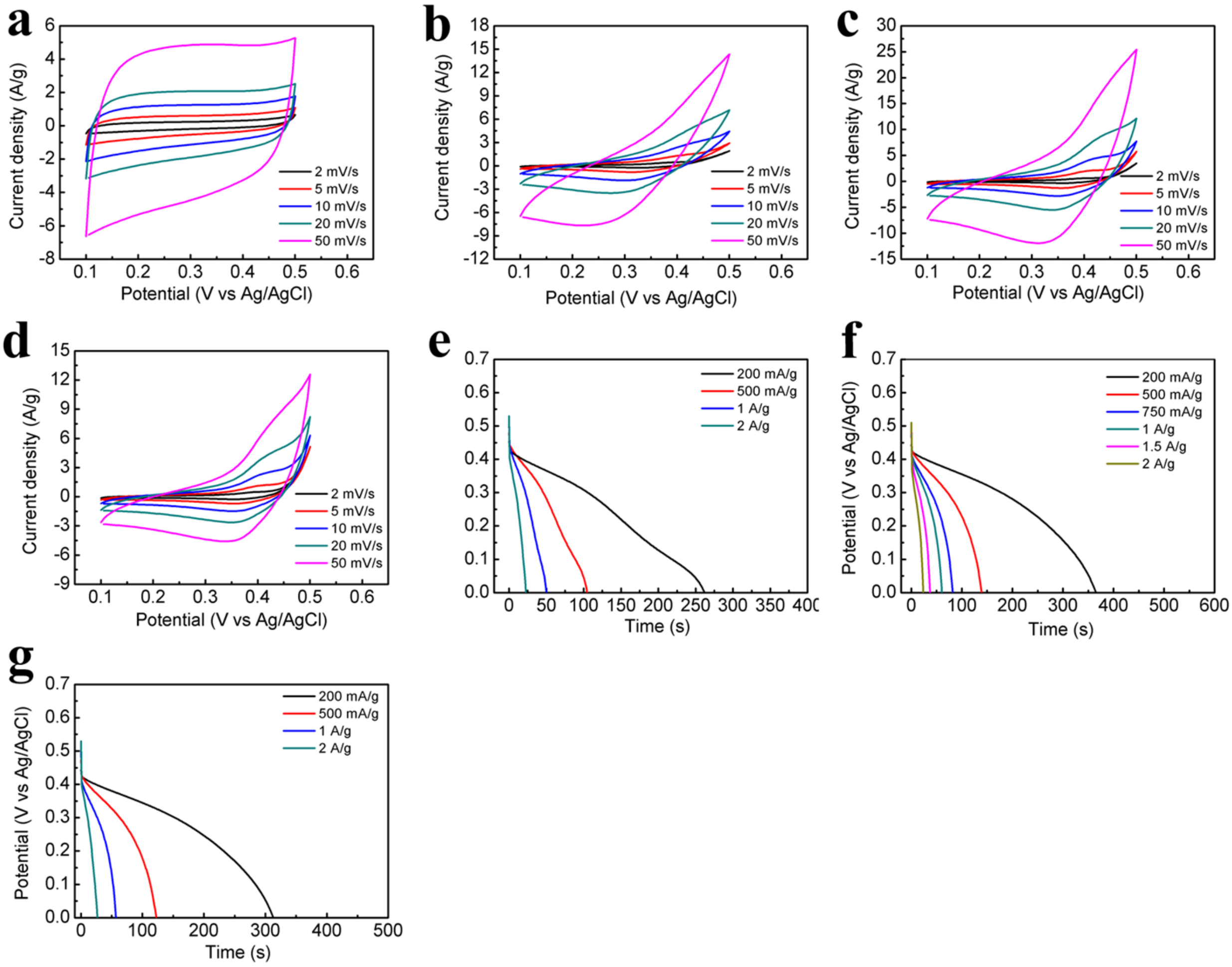

Fig. S4 Cyclic voltammetric curves of α-MnO_2 nanotube (a), MnO_2@Co_3O_4-H (b), MnO_2@Co_3O_4-L (c) and MnO_2+Co_3O_4 (d) at different scan rates; galvanostatic discharge curves of α-MnO_2 nanotube (e), MnO_2@Co_3O_4-H (f) and MnO_2+Co_3O_4 (g) at different current densities.